

1 **Spindle F-actin coordinates the first metaphase-anaphase transition in *Drosophila* meiosis**

2 Benjamin W. Wood and Timothy T. Weil[‡]

3 Department of Zoology, University of Cambridge, Downing Street, Cambridge, CB2 3EJ, UK

4 [‡]Author for correspondence (e-mail: tw419@cam.ac.uk)

5 **ABSTRACT**

6 Meiosis is a highly conserved feature of sexual reproduction that ensures germ cells have the correct
7 number of chromosomes prior to fertilization. A subset of microtubules, known as the spindle, are
8 essential for accurate chromosome segregation during meiosis. Building evidence in mammalian
9 systems has recently highlighted the unexpected requirement of the actin cytoskeleton in
10 chromosome segregation; a network of spindle actin filaments appear to regulate many aspects of
11 this process. Here we show that *Drosophila* oocytes also have a spindle population of actin that
12 regulates the formation of the microtubule spindle and chromosomal movements throughout
13 meiosis. We demonstrate that genetic and pharmacological disruption of the actin cytoskeleton has
14 a significant impact on spindle morphology, dynamics, and chromosome alignment and segregation
15 during the metaphase-anaphase transition. We further reveal the requirement of calcium in
16 maintaining the microtubule spindle and spindle actin. Together, our data highlights the significant
17 conservation of morphology and mechanism of the spindle actin during meiosis.

18 INTRODUCTION

19 Meiosis is a well studied and documented process that is essential for the production of haploid
20 gametes during sexual reproduction. In mammals, fetal oogonia initiate meiosis synchronously,
21 arresting at prophase I and pausing in this state until sexual maturity, whereupon an oocyte or small
22 subsets of oocytes are released periodically and meiosis is resumed¹. Nuclear envelope breakdown
23 initiates this resumption, resulting in the formation of a bipolar spindle network as microtubules
24 polymerize, capture chromosomes and then align them on the metaphase plate². The spindle
25 interacts closely with the cytoplasmic actin, which aids in the asymmetric positioning of the spindle
26 adjacent to the cortex, enabling asymmetric cell division to leave a single oocyte containing the
27 necessary maternal components²⁻⁷. Oocytes are arrested in metaphase II until fertilization and
28 subsequent egg activation. An intracellular calcium rise then triggers the completion of meiosis,
29 resulting in the formation of the maternal pronucleus which undergoes fusion with the paternal pro-
30 nucleus to form a diploid zygote^{8,9}.

31 In *Drosophila melanogaster*, the process is similar but with a few key differences. Oocytes are
32 generated continuously when environmental conditions are favorable. Connected to supporting cells
33 via cytoplasmic bridges and surrounded by a mono-layer of epithelial cells, the oocyte passes
34 through morphologically distinct stages during oogenesis. Meiosis is held in late prophase I for the
35 majority of oogenesis, until the prophase-metaphase transition^{10,11}. Key features of this step can be
36 observed within the *Drosophila* oocyte, such as nuclear envelope breakdown and formation of a
37 bipolar spindle as microtubule spindles capture the meiosis I chromosomes^{12,13}.

38 Unlike mammals and most vertebrates, the final arrest in *Drosophila* oocytes is at metaphase I, and
39 the bipolar spindle structure that forms is more defined and has more focused spindle poles when
40 compared to the “barrel” shaped spindles of mammals. Activation in *Drosophila* occurs prior to
41 fertilization as the oocyte passes into the oviduct, resulting in calcium influx through transient
42 receptor potential melastatin (TrpM) ion channels in the plasma membrane of the oocyte^{14,15}. This
43 calcium event enables the resumption of meiosis from its arrested state, and can be observed using
44 a variety of microtubule labelling tools¹⁶. Detailed cytological studies of *Drosophila* oocytes revealed
45 that at the metaphase I arrest, the chromosomes exist as a central mass, including the non-
46 exchange chromosomes, which can be visible as a separate entity during pro-metaphase or
47 anaphase^{16,17}. The metaphase to anaphase transition is described as a stereotypical series of
48 events; 1) the meiotic spindle elongates; 2) then contracts, decreasing in length but increasing in
49 width; 3) the meiotic spindle then rotates in relation to the cortex resulting in a perpendicular
50 orientation to the cortex¹⁶. Identification of *Drosophila* oocytes at metaphase I arrest is easily
51 observable through the developmental stage of the dorsal appendages, which at a length of greater
52 than 250 μm indicate the mature oocyte¹⁷.

53 The mature *Drosophila* oocyte itself is approximately 500 μm in length, compared to the spindle
54 which is approximately 10 μm (~50:1 ratio of oocyte to spindle). In contrast, the mouse oocyte has
55 a ratio of approximately 5:1 oocyte to spindle length¹⁸. The *Drosophila* oocyte itself is vitellogenic
56 and surrounded by protective outer casings, reflecting the need for the oocyte to be as robust as
57 possible as they ultimately develop external to the organism. These features can initially make
58 distinguishing the components of the *Drosophila* spindle challenging. However, with the plethora of
59 genetic tools available, visualization and manipulation of spindle components can now be easily
60 achieved, highlighting *Drosophila* as an important model system for understanding and future
61 research of this field.

62 Recently, it has been observed that a population of actin exists within the mammalian oocyte that
63 forms a spindle-like structure and has been shown to regulate chromosome alignment and
64 segregation¹⁸. Treatment of these oocytes with cytochalasin D (cytoD) and knockout of Formin-2, a
65 key nucleator of spindle-like actin in mice, results in the misalignment of chromosomes during
66 metaphase I and chromosome segregation errors during anaphase, often resulting in aneuploidy.
67 Actin was shown to regulate chromosomal movements in part due to control of the kinetochore
68 microtubules (K-fibres), indicating a likely role of actin in microtubule organization more generally¹⁸.
69 Multi-color 3D-fluorescence microscopy revealed that human oocytes display a population of spindle
70 actin similar to the population in mice, and additionally demonstrated that there is co-localization of
71 γ -tubulin rich minus ends with filamentous actin clusters at the spindle poles¹⁹. Pharmacological
72 manipulations revealed a co-operation of actin and microtubules at the meiotic spindle, as disruption
73 of the microtubule spindle morphology is directly mirrored by changes to the spindle actin. Taken
74 together, this data suggests that the spatiotemporal organization of actin during oocyte maturation
75 follows microtubule dynamics.

76 In this study, we utilize advanced imaging in conjunction with pharmacological and genetic
77 manipulation to demonstrate that a population of spindle actin exists in the metaphase I arrested
78 mature *Drosophila* oocyte. We show that the mammalian Formin-2 homologue, Cappuccino (Capu),
79 is required for the formation of the spindle actin network, which undergoes strikingly similar
80 morphological changes to the microtubule spindle during egg activation. Disruption of this network
81 reveals that actin is required for regulating the alignment and segregation of chromosomes during
82 meiosis. Moreover, visualization and manipulation of calcium ions at this transition reveals the
83 importance of calcium signaling for maintaining the morphology of the metaphase spindle and
84 chromosome segregation. Taken together, our data suggests that actin is required upstream of the
85 microtubules to regulate formation of the spindle.

86 RESULTS

87 Actin is present at the spindle

88 Mature *Drosophila* oocytes are arrested at metaphase I and held within the ovaries. Ovulation then
89 triggers egg activation during which the metaphase-anaphase transition occurs. The metaphase
90 arrested microtubule spindle can be visualized with the microtubule binding protein Jupiter (Jup)
91 fused to GFP (Jup-GFP) as a comparatively small structure in relation to the rest of the oocyte (Fig.
92 1a), and lies parallel to the cortex at the dorsal-anterior tip of the oocyte, just below the dorsal
93 appendages. The microtubule spindle forms an elliptical structure with focused poles, with the
94 chromosomes lying centrally in this structure (Fig. 1a, b). It is often the case that the 4th non-
95 exchange chromosomes are visible as a smaller mass at each tip of the main body of chromosomes.
96 Surrounding the oocyte is a layer of follicle cells, which are required during oogenesis for patterning
97 of the oocyte. The follicle cell nuclei are clearly visible in this layer, encompassing the oocyte (Fig.
98 1a).

99 We first sought to test if the recently established novel population of actin within the spindle in mouse
100 and human oocytes, is conserved in *Drosophila* oocytes^{18,19}. We used two genetically-encoded actin
101 markers: Act5C-GFP, the actin 5C monomer conjugated to a GFP²⁰; and Lifeact-GFP, the actin
102 binding protein Lifeact conjugated to a GFP that has been well-established as a faithful actin label
103 in *Drosophila*²¹. These were expressed in the female germ-line, and mature oocytes were fixed and
104 stained with diamidino-2-phenylindole (DAPI) (Fig. 1c, d). A distinct spindle-like population of actin
105 can be observed using both Act5C-GFP and Lifeact-GFP, with the metaphase chromosomal mass
106 localizing to the center of these structures.

107 This result was also shown live using the calponin-homology domain of Utrophin (Utr), required for
108 the actin binding capacity of Utr, conjugated to an enhanced green fluorescent protein (GFP) (UtrCH-
109 GFP) expressed in the *Drosophila* female germline. This tool has been used previously in other
110 systems to successfully label the spindle actin for live analysis¹⁸. Utilizing high-resolution confocal
111 microscopy at the dorsal-anterior tip of the oocyte revealed the existence of a small but highly distinct
112 population of actin (Fig. 1e). This actin resembles closely the microtubule spindle as it forms an
113 elliptical shape with focused poles (a unique feature of the *Drosophila* meiotic spindle), and will
114 henceforth be referred to as spindle actin. We then tested whether this population of spindle actin
115 required Capu, the mammalian Formin-2 homologue, for formation. Live visualization of UtrCH-GFP
116 was performed in a *capu* heterozygous background, specifically using *capu*^{EY12344}, a hypomorphic
117 mutant generated through insertion of a P-element into the first common exon²²⁻²³. This was sufficient
118 to disrupt the formation of this spindle actin population, with a significant proportion of oocytes not
119 displaying a spindle actin network whatsoever (Fig. 1f).

120 Together, this establishes a spindle actin population in *Drosophila* and, consistent with mammals,
121 that the Capu protein is required for accurate formation of the spindle network surrounding the
122 congressed metaphase chromosomes.

123 **Spindle-like actin regulates metaphase spindle microtubules and chromosomes**

124 To test the function of spindle actin, we first examined the relationship between this actin population
125 and the microtubule spindles. Oocytes expressing Jup-GFP that were incubated in the microtubule
126 depolymerizing agent colchicine showed a complete loss of the microtubule spindle (Fig. 2a).
127 However, the spindle actin (UtrCH-GFP) remained in the presence of colchicine (Fig. 2b), suggesting
128 this population is resistant to disruption of the spindle microtubules. Inversely, depolymerization of
129 the actin cytoskeleton using cytoD resulted in an elongated morphology of the microtubule spindle,
130 as well as the expected loss of spindle actin (Fig. 2c and 4b). To more directly target the spindle
131 actin, we visualized Jup-GFP in mutant backgrounds of *capu* and *spire*, which act as part of a Capu-
132 Spire actin nucleating complex (Fig. 2d-f). In both heterozygous and trans-heterozygous mutant
133 oocytes, the spindle appeared significantly elongated (Fig. 2g). Furthermore, in *capu* trans-
134 heterozygous backgrounds we observe a significant increase in the number of oocytes without
135 spindle microtubules (Fig. 2h).

136 Next, we used fluorescence recovery after photobleaching (FRAP) to test the dynamics of
137 microtubule recruitment in wild-type and *capu/spire* trans-heterozygous oocytes. When the spindle
138 actin is disrupted, we observed a significant change in the recovery dynamics of the microtubule
139 spindle (Fig. 2i). The failure of the spindle to recover fluorescence to a wild-type level, suggests the
140 spindle actin population plays a role in the recruitment of microtubules to the spindle itself. Taken
141 together, our analyses reveal an important relationship between the spindle actin and microtubule
142 spindle, as actin is required for accurate formation of the microtubule spindle and regulation of its
143 morphology. This appears conserved with studies in mice and humans, in which the spindle actin
144 has been shown to be required for formation of K-fibres and recovery of the spindle structure^{18,19}.

145 Considering the function of the microtubule spindle in chromosome segregation, we next tested if
146 the spindle actin is involved in this process. We, therefore, observed chromosome alignment within
147 the metaphase-arrested spindle after disruption of actin. Prior to metaphase, the chromosomes lie
148 in a centrally congressed mass surrounded by the spindle actin (Fig. 3a), however, following
149 treatment with cytoD (Fig. 3b), there is significant disruption to the alignment of these chromosomes.
150 We detect multiple chromosomal masses spreading to either pole of the spindle axis. Similarly, in
151 *capu* and *spire* mutant genetic backgrounds, clear disruption to the centrally congressed
152 chromosomal mass can be observed (Fig. 3c, d). Measuring this spread of the metaphase I
153 chromosomes as the maximum chromosomal distance reveals a significant increase in those
154 oocytes with a disrupted spindle actin (Fig. 3e). Furthermore, analysis of the angle the spindle makes
155 with the cortex reveals a significant change when actin is disrupted (Fig. 3f). Together this suggests

156 that this population of actin is required to promote and maintain the compact nature of the
157 chromosomes centrally, without which misalignment of the chromosomes and spindle occurs.

158 **Functional importance of the spindle actin during anaphase I**

159 In order to test if the functional importance of this actin population extends throughout meiosis, we
160 observed the spindle actin during egg activation. In *Drosophila*, egg activation occurs as the oocyte
161 passes into the oviduct, but can be recapitulated *ex vivo* through incubation in a hypotonic buffer
162 (activation buffer (AB)) which causes the egg to swell. This results in TrpM calcium ion channels
163 opening which enables a calcium transient to pass through the cell and initiate the metaphase-
164 anaphase transition^{14,15}. Microtubule spindles undergo a classical rearrangement at egg activation
165 as the spindle initially elongates, then contracts and rotates in relation to the cortex, ultimately
166 becoming perpendicular to the cortex by meiosis II (Fig 3g). Observation of the spindle actin during
167 egg activation reveals a similar morphological change, as the spindle actin ultimately contracts (Fig.
168 3h). This is highly reminiscent of the morphological change observed with the microtubules at egg
169 activation. This suggests that the interplay between spindle actin and the microtubule spindle
170 continues in anaphase I.

171 We next tested the role of the actin cytoskeleton during anaphase. Fixation of activated oocytes
172 revealed co-localization of the anaphase I chromosomes with a filamentous and spindle-like
173 population of actin (Fig. 4a). Disruption of the anaphase spindle actin was achieved through
174 treatment with cytoD following AB treatment to ensure oocytes had entered anaphase. This resulted
175 in significant disruption to the segregation of the chromosomes, with frequent occurrence of aberrant
176 chromosomal masses, which we define as chromosomes completely separate from the main axis of
177 segregating chromosomes or a mass causing obvious non-uniformity (Fig. 4b, c). Similarly,
178 visualization of the chromosomes in *capu* heterozygous and *capu/spire* trans-heterozygous
179 backgrounds revealed aberrations in chromosome segregation (Fig. 4d-g). Individual aberrant
180 chromosomal masses were clearly identifiable, with all test oocytes demonstrating a significant
181 increase in the number of these masses as compared to wild type oocytes (Fig. 4h). Furthermore,
182 in the case of *capu/spire* trans-heterozygous oocytes, it was common to observe the 4th non-
183 exchange chromosomes being closely located, suggesting a loss of spindle polarity (Fig. 4g).
184 Despite clear loss of accurate segregations, measurements of the maximum chromosomal distances
185 did not reveal any significant differences from control oocytes, suggesting chromosome segregation
186 was still able to occur, but with a loss of accuracy (Fig. 4i). In addition, we observed no significant
187 difference in the angle of the spindle-cortex between cytoD treated oocytes in anaphase versus
188 anaphase controls and cytoD treated metaphase oocytes (Fig. 4j). We do, however, still observe a
189 significant increase in the angle as compared to metaphase, with the most significant increase for
190 cytoD treated anaphase oocytes. Together, this demonstrates that many anaphase events are still
191 capable of occurring when the spindle actin is disrupted, including chromosome segregation and
192 spindle rotation. It therefore suggests that the main role of the spindle actin is in providing a level of

193 accuracy to these events, as without it we see dramatic aberrations in the quality of chromosome
194 segregation.

195 **Localized calcium signaling may be required at the spindle for effective meiosis**

196 Previous work has shown a clear link between calcium and actin at and around egg activation²⁴.
197 Recent evidence in mature *Xenopus* oocytes also highlights the presence of enriched calcium and
198 necessity of localized calcium signaling at the spindle for regulation of microtubules²⁵.

199 We used a genetically encoded calcium sensor, GCaMP3, to visualize calcium *in vivo*²⁶. Increased
200 fluorescence intensity at the spindle was observed with live and fixed imaging, indicating a calcium
201 enrichment (Fig. 5a, b). Interestingly, there appears to be the greatest enrichment at the tip of each
202 pole of the spindle in the metaphase oocyte, compared to a more uniform signal in the anaphase
203 oocyte, yet this still suggests a requirement throughout egg activation.

204 To test the role of calcium at the spindle, mature oocytes were incubated in the membrane permeable
205 calcium chelating agent BAPTA-AM. The removal of calcium results in the loss of both an actin and
206 microtubule spindle population, suggesting that calcium signaling is required to maintain the spindle
207 apparatus (Fig. 5c, d). This is similar to results in *Xenopus* in which BAPTA incubation caused
208 microtubule depolymerization in a similar fashion to microtubule depolymerizing agents²⁵.
209 Furthermore, BAPTA-AM incubations result in the complete compaction of the chromosomes into
210 one rounded mass (Fig. 5e). This phenotype is likely explained by the previous results in which
211 BAPTA causes complete loss of the microtubules and actin within the spindle.

212 Finally, disruption of the spindle actin through introduction of the *capu*^{EY12344} mutant resulted in a loss
213 of enrichment of calcium at the spindle (Fig. 5f). As expected, the chromosomes become separated
214 into two individual masses that begin to separate toward spindle poles. However, the enrichment of
215 the GCaMP3 can no longer be observed. Together this shows that calcium is required for the
216 maintenance of the spindle apparatus at metaphase, with an interdependence becoming apparent
217 between the spindle actin and calcium signaling.

218 **DISCUSSION**

219 This study establishes the existence of a population of spindle-like F-actin in *Drosophila* mature
220 oocytes that is required for the regulation of meiosis. We demonstrate the requirement of the
221 mammalian homologue of Formin-2 in the formation of this spindle actin. Disruption of the actin
222 spindle results in dramatic chromosome segregation errors. At metaphase, the spindle lacks
223 accurate chromosome alignment and congression, and at anaphase aberrant chromosomal masses
224 are frequent. We also identify calcium as critical in maintaining the spindle throughout metaphase.
225 Together, we suggest that the spindle actin is required to mediate the accurate segregation of
226 chromosomes through regulation of the microtubule spindle. Our data, together with recent work that
227 reveals a population of spindle actin in mammals^{18,19} and calcium enrichment in *Xenopus*²⁷, suggests
228 there is a high level of evolutionary conservation at the spindle.

229 The conservation, from mammals to *Drosophila*, we see in both functional and morphological
230 similarities between spindle actin populations. Whilst variation is to be expected in comparison of
231 meiotic mechanisms between species, such as final meiotic arrest occurring at metaphase I in
232 *Drosophila*, in comparison to metaphase II in mammals, it appears that distinct populations of spindle
233 actin may be another fundamental feature of meiosis. The conservation of this population of actin
234 extends from its nucleation by the Formin-2 homolog Capu, to its functional role in the regulation of
235 spindle microtubules and chromosomal movements.

236 However, there does appear to be some variation in the morphology and function of this spindle
237 population. Much like the microtubule spindle, the spindle actin forms an elliptical shape with highly
238 focused poles, unlike mammalian meiotic spindle structures which are more 'barrel like' in shape².
239 This population also seems to be resilient to disruption of the microtubule spindle, appearing to be
240 important for recruitment of microtubules to the spindle and regulating overall spindle morphology,
241 therefore suggesting an upstream requirement of the actin cytoskeleton. When disrupted, either
242 through knockdown of *capu* or depolymerization by cytoD, significant defects in chromosome
243 alignment can be observed. Observation of metaphase I oocytes indicated a spreading of the
244 chromosomes along the metaphase spindle, with separation of chromosomes appearing reminiscent
245 of pro-metaphase oocytes¹⁷. This could suggest a requirement of the spindle actin in the prophase-
246 metaphase transition, a much earlier stage than has been observed in mammals to date. Perhaps
247 this population of actin plays a more significant role in *Drosophila* meiosis I as mature oocytes arrest
248 at metaphase I, which may indicate that the actin is important in meiotic arrest and release from this
249 arrest during egg activation and onset of the metaphase-anaphase transition.

250 During egg activation, a global transient of calcium triggers a plethora of events, including global
251 rearrangements of the actin cytoskeleton and resumption of meiosis²⁴. There is building evidence
252 that ties calcium and actin as two interlinked molecules in many signaling pathways; in *Drosophila*
253 egg activation, dispersion of cortical actin enables entry of calcium in the form of a wave, which,

254 downstream, effects a wave of reorganizing F-actin²⁴. With many actin binding proteins (ABPs) being
255 calcium sensitive, such as α -actinin and the villin family, and many calcium-sensitive proteins having
256 downstream effects on the actin cytoskeleton, such as Calmodulin and calcineurin²⁸, it is very
257 probable that the calcium wave has a direct effect on the population of spindle actin, potentiating the
258 release from meiotic arrest.

259 We have observed directly an enrichment of the calcium indicator GCaMP3 at the metaphase
260 arrested spindle, suggesting an increased local concentration of calcium. When calcium is removed,
261 depolymerization of the actin and microtubule spindles can be observed, indicating the requirement
262 of calcium in maintenance of these populations, consistent with observations in *Xenopus*²⁵. Our data
263 suggests an interdependent relationship with the spindle actin and calcium, as it appears that
264 enrichment of the calcium signal is reduced in *capu* mutants. This may suggest the presence of
265 localized calcium signaling between the spindle actin and associated ABPs and/or that the actin aids
266 in recruitment of calcium-sensitive proteins more generally within the spindle. More complete
267 knockdown of *capu* often results in the loss of formation of the microtubule spindle, furthering an
268 argument in which the spindle actin is required for recruitment of microtubules. This recruitment could
269 be direct, but given the requirement of calcium for formation and maintenance of spindle populations,
270 it is likely that the loss of actin may impact the formation of microtubules through disruption of the
271 localized action of many calcium sensitive proteins. One family of candidates is the microtubule
272 associated proteins (MAPs), many of which are calcium sensitive and associate with both the actin
273 and microtubule cytoskeleton²⁷. Without the spindle actin, it is likely that the localization and
274 coordination of these proteins are lost, resulting in a loss of calcium signaling at the spindle and
275 concomitant loss of the microtubule spindle itself. Given the ubiquitousness of calcium at the spindle,
276 this mechanism should be explored further in mammals, as it is likely another conserved feature of
277 meiosis.

278 **ACKNOWLEDGEMENTS**

279 We are grateful to Jens Januschke, Torsten Krude, Jose Casal, and Paul Conduit for discussions
280 and advice; Elise Wilby for feedback on the manuscript; the Zoology Imaging Facility and Matt
281 Wayland for assistance with microscopy; the Bloomington *Drosophila* Stock Center and *Drosophila*
282 community for fly lines.

283 **AUTHOR CONTRIBUTIONS**

284 B.W.W. was responsible for conceptualization, methodology, experimentation, analysis, and writing.
285 T.T.W was responsible for conceptualization, supervision, and reviewing.

286 **COMPETING INTERESTS**

287 The authors report no competing interest.

288 MATERIALS AND METHODS

289 Fly Maintenance

290 Fly stocks were raised on Iberian recipe fly food at 18°C, 21°C and 25°C. For dissection of mature
291 oocytes, approximately 30 female flies with 5 male flies were transferred into a vial with Iberian recipe
292 fly food and wet yeast for 48 hours at 25°C.

293 Fly lines

294 *mata-GAL4::VP16, UASp-GCaMP3*²⁹; *tub-GAL4VP16* (S. Roth); *UASp-Utrophin-CH-GFP/Tm3*³⁰;
295 *UASp-LifeactGFP/Tm3* (BL58717); *UASp-Act5CGFP/Tm3* (BL7309); *P{PTT-GA}JupiterG00147*
296 (BL6836); *P{PTT-un}CamP00695/CyO* (BL50843); *capu*^{EY12344}³⁰; *capu*^{EE}/*CyO* (BL8788);
297 *spire*^{2F}/*CyO* (BL8723).

298 Preparing oocytes for live imaging

299 Ovaries from flies fattened for 48 hours on yeast were dissected onto a 22 by 40 mm cover slip, into
300 series 95 halocarbon oil using forceps (11251-30 Dumont #5 forceps, Fine Science Tools) and a
301 dissecting probe (0.25 mm straight 10140-01, Fine Science Tools) as described previously³¹. Mature
302 oocytes were gently teased out of the ovaries and left for 10 minutes prior to imaging to allow them
303 to settle onto the coverslip.

304 Preparing *in vivo* activated eggs

305 Ovaries from flies fattened for 48 hours on yeast were carefully dissected onto a 22 by 40mm cover
306 slip, such that the oviduct was still intact, into series 95 halocarbon oil. Oocytes were then gently
307 teased out of the oviduct, carefully removing the surrounding oviduct tissues.

308 Preparation of fixed samples

309 Ten to twenty ovaries were dissected from flies fattened for 48 hours on yeast into Schneider's Insect
310 Medium (Sch) (GibCo). Ovaries were splayed open and oocytes gently teased out using fine forceps
311 (11251-30 Dumont #5 forceps, Fine Science Tools) and a dissecting probe (0.25 mm straight 10140-
312 01, Fine Science Tools). Mature oocytes were transferred into an 0.5mL eppendorf tube using a
313 glass pipette. Sch was removed and 500 µL 4% paraformaldehyde (PFA) stabilized with phosphate
314 buffer (ThermoFisher Scientific) was added for 10-15 minutes on a rotary machine (PTR-35 360
315 vertical multi-function rotator, ThermoFisher Scientific). Oocytes were then washed for 10 minutes,
316 three times in 0.1% PBST (0.1% Triton X-100 (ThermoFisher Scientific) in PBS. Oocytes were then
317 incubated for 2 hours in 1% PBST with the following labelling probes, before washing, staining in
318 glycerol and DAPI and mounting on a glass slide in Vectashield with DAPI (Vector Laboratories):
319 Alexa-Fluor Phalloidin 568, 1:500 (Molecular Probes); Alexa-Fluor Phalloidin 637, 1:500 (Molecular
320 Probes); ChromoTek GFP-booster, 1:500 (Proteintech).

321 *Ex vivo* egg activation

322 Mature oocytes were activated *ex vivo* through addition of the hypotonic, 260 mOsm, activation
323 buffer (AB): 3.3 mM NaH₂PO₄, 16.6 mM KH₂PO₄, 10mM NaCl, 50 mM KCl, 5% polyethylene glycol
324 (PEG) 8000, 2mM CaCl₂, brought to pH 6.4 with a 1:5 ratio of NaOH:KOH³². Oocytes typically
325 activate within two minutes of addition of AB.

326 **Pharmacological treatments**

327 All pharmacological incubations were validated with either a Schneider's Insect Medium (Sch) or
328 PBS control and a DMSO control made to the appropriate dilution. Oocytes were incubated in Sch
329 or PBS for 10 minutes whereupon samples were flooded with AB and visualized.

330 CytoD (Sigma Aldrich) was made to a final concentration of 2-20 μM in Sch or PBS. Oocytes were
331 dissected into Sch or PBS a glass bottom dish. The Sch or PBS was carefully removed and replaced
332 with the cytoD. Oocytes were incubated for 10 to 30 minutes in this solution prior to fixation or live
333 imaging. Colchicine (Sigma Aldrich) was made to a final concentration of 50 μM in Sch or PBS.
334 Oocytes were incubated for at least 30 minutes in this solution prior to fixation or live imaging, as
335 above.

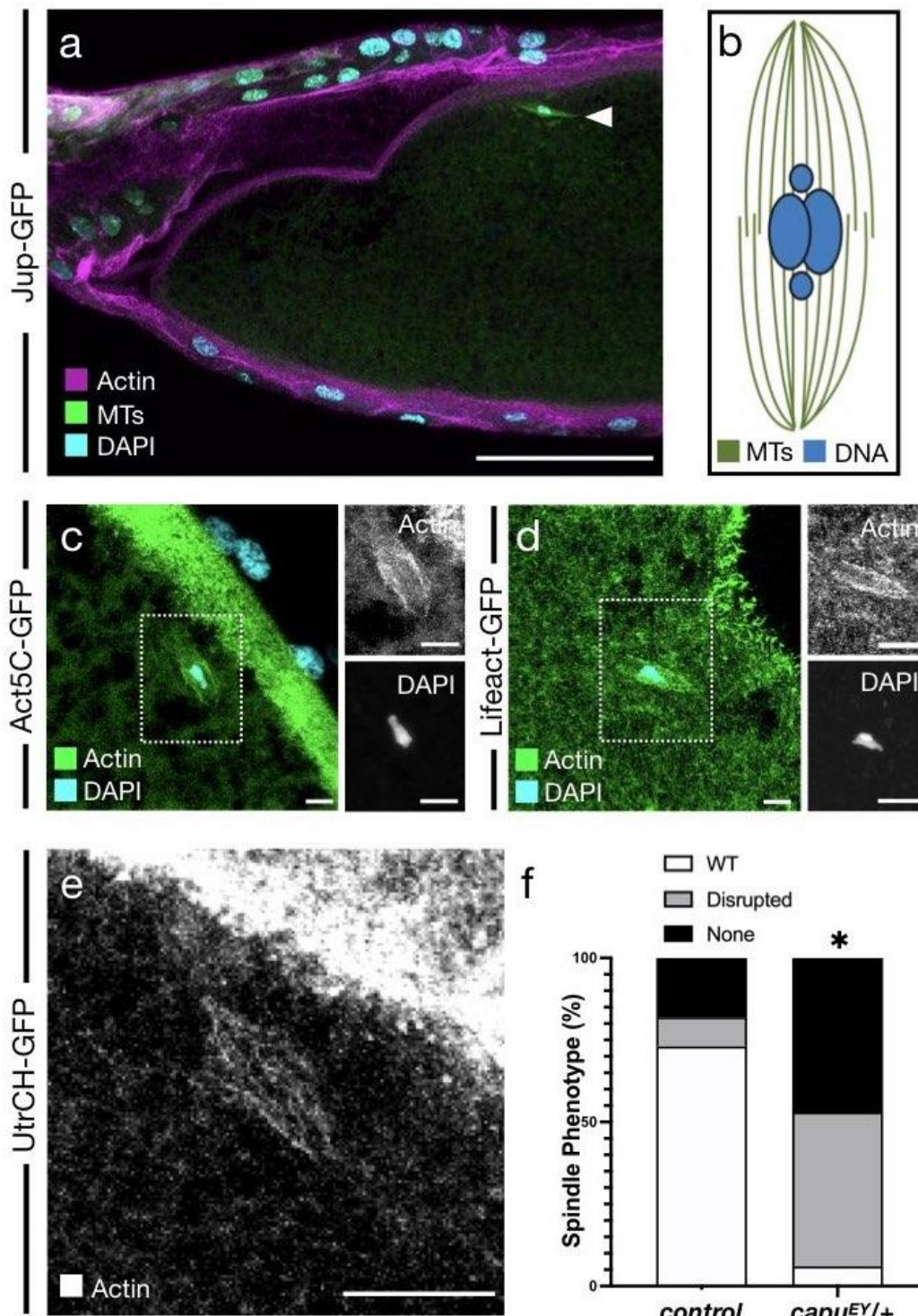
336 **Imaging with the Inverted Olympus FV3000 system**

337 An 1.05 NA 30X silicone objective was used for whole oocyte imaging and an 1.35 NA 60X silicone
338 objective for visualizing intracellular components. For high resolution imaging of the spindle, oocytes
339 were oriented on the coverslip such that the dorsal appendages were in contact with the surface of
340 the cover slip, therefore the dorsal side of the oocyte becomes the shallowest plane of visualization.
341 Parameters for image collection were: 1.35 NA 60x silicon immersion objective, 10 μm Z-stack,
342 0.5 μm between each Z-slice, 1024×1024 pixels, approximately 15 seconds per stack.

343 **FRAP analysis**

344 For FRAP of spindle components Jup-GFP was bleached for 10 seconds. Time lapse series of
345 recovery was recorded every 5 seconds in single plane imaging of the cortex or every 30 seconds
346 in Z-stack imaging of the spindle, both using the 488nm laser channel, 2 Airy unit pinhole, 1024x1024
347 pixels. For all FRAP series, background correction was performed by subtracting the fluorescence
348 intensities of the unbleached cytoplasmic area from fluorescent intensities of bleached regions, with
349 percentage fluorescence of the maximum plotted in graphs.

350 **FIGURE 1**



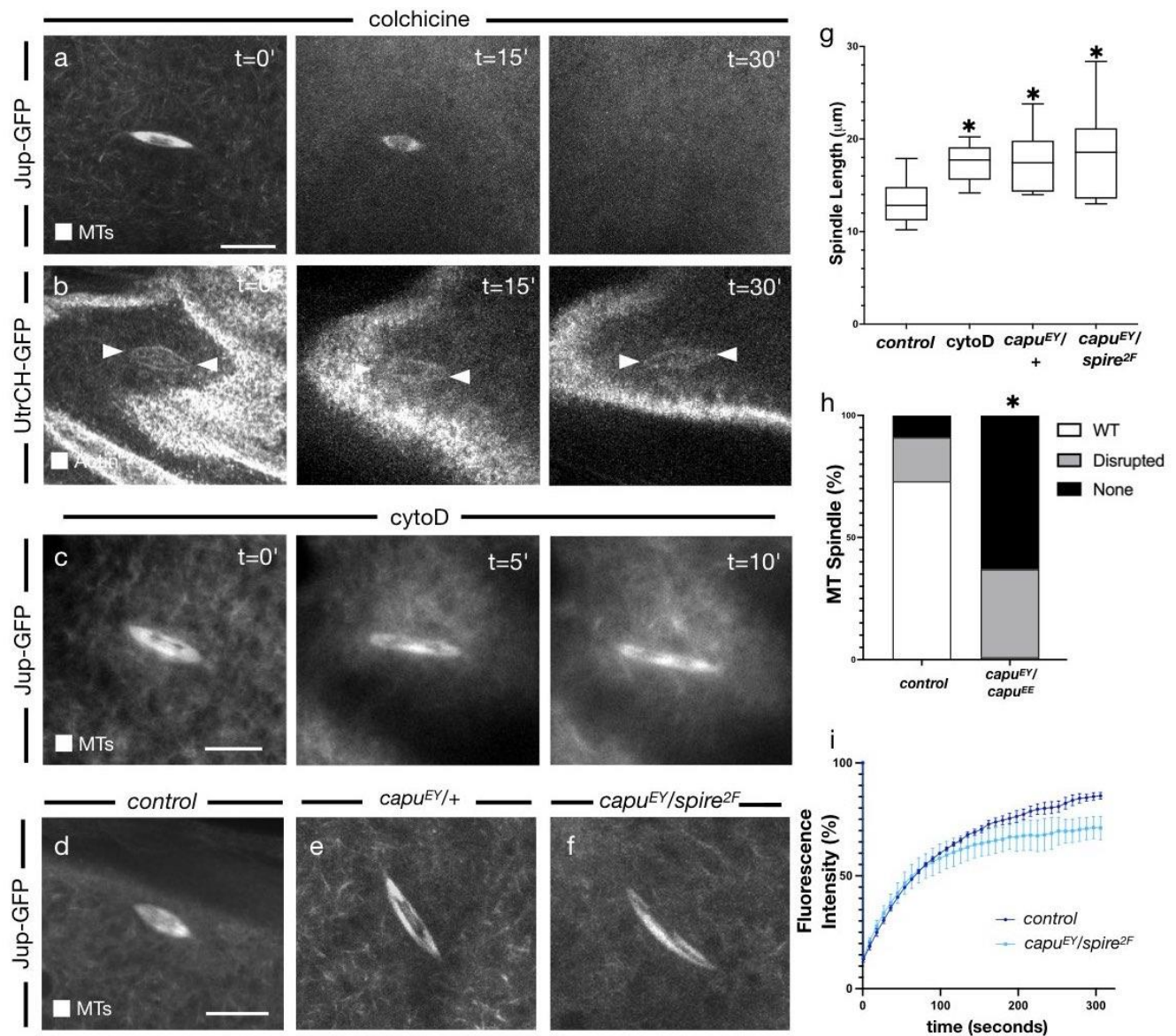
351 **Fig. 1** A spindle-like actin population in the metaphase-arrested *Drosophila* mature oocyte.

352 a. Confocal Z-projection (40 μ m) of a fixed metaphase I (MI) oocyte. Microtubules shown in green
353 (Jup-GFP, GFP-booster), Actin shown in magenta (Alexa-fluor568 Phalloidin), DNA shown in
354 cyan (DAPI). Spindles (white arrowhead) lie parallel to the dorsal-anterior cortex of the oocyte.

355 b. Schematic representing the MI arrested spindle in the *Drosophila* oocyte. Microtubules (MTs)
356 are represented in green and the metaphase chromosomal mass is represented in blue. Spindle

- 357 forms with highly focused poles with four centrally located chromosomes. Fourth non-exchange
358 chromosomes appears as a distinct unit at the polar tips of the mass.
- 359 c. Confocal Z-projection (10 μm) of a fixed MI oocyte. Merge shows actin (Act5C-GFP) in green,
360 DNA (DAPI) in cyan, demonstrating a spindle-like population of actin surrounding a central
361 chromosomal mass. Dashed-line box marks region that is magnified in single-color images to
362 right.
- 363 d. Confocal Z-projection (10 μm) of a fixed MI oocyte. Merge shows actin (Lifeact-GFP) in green,
364 DNA (DAPI) in cyan, demonstrating a spindle-like population of actin surrounding a central
365 chromosomal mass. Dashed-line box marks region that is magnified in single-color images to
366 right.
- 367 e. Confocal Z-projection (10 μm) of a live MI oocyte. This population of actin (UtrCH-GFP) appears
368 as a spindle-like structure, with filaments traversing the spindle.
- 369 f. Comparison of the spindle phenotypes for *wild-type* and *capu*^{EY12344}/₊ heterozygous mutant
370 shows a significant increase in the percent of oocytes showing elongated or no spindle. N = 25,
371 * <0.05 , Fishers Exact Test.
- 372 Scale bar: 50 μm (a), 5 μm (c,d), 10 μm (e).

373 **FIGURE 2**



374 **Fig. 2** Actin cytoskeleton promotes recruitment of spindle microtubules and regulation of spindle
 375 morphology.

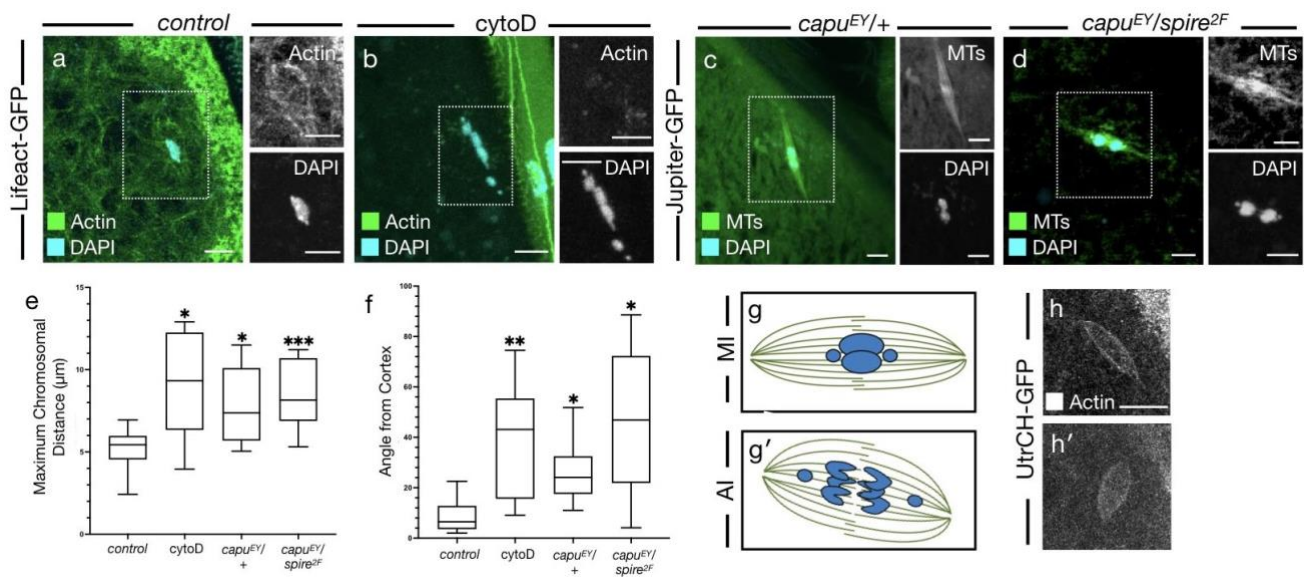
376 a. Confocal Z-projections (10 μm) from a live time series of a MI oocyte treated with colchicine
 377 ($t=0'$). Microtubules (Jup-GFP) first appear as a typical spindle structure and completely
 378 depolymerize post-treatment ($t=30'$). N = 5.

379 b. Confocal Z-projections (10 μm) from a live time series of a MI oocyte treated with colchicine
 380 ($t=0'$). Spindle-like actin (UtrCH-GFP) remains unchanged post-treatment ($t=30'$). N = 5.

381 c. Confocal Z-projections (10 μm) from a live time series of a MI oocyte following incubation with
 382 the 10 μM of the actin depolymerizing agent cytoD. Before addition ($t=0'$), the spindle (Jup-GFP)
 383 appears as a typical elliptical structure of approximately 10 μm . Post-cytoD addition ($t=10'$), the
 384 spindle has undergone a distinct morphological change as it elongates significantly. Scale bar
 385 represents 10 μm . N = 9.

- 386 d. Confocal Z-projections (10 μm) from a live MI oocyte. Microtubules (Jup-GFP) appear as the
387 typical spindle structure. N = 20.
- 388 e. Confocal Z-projection (10 μm) from a live *capu*^{EY12344}/+ heterozygous mutant MI oocyte.
389 Microtubules (Jup-GFP) appear as an elongated spindle. N = 20.
- 390 f. Confocal Z-projection (10 μm) from a live *capu*^{EY12344}/*spire*^{2F} trans-heterozygous mutant MI
391 oocyte. Microtubules (Jup-GFP) appear as an elongated spindle. N = 20.
- 392 g. Comparison of the microtubule spindle length indicates a significant increase in cytoD treated
393 and mutant backgrounds compared to wild-type. * < 0.05, N = 25, student's t-test.
- 394 h. Comparison of the spindle phenotypes for wild-type and *capu*^{EY12344}/*capu*^{EE} trans-heterozygous
395 mutant shows a dramatic increase in the percent of oocytes without a spindle. N = 20, * < 0.05.
- 396 i. Recovery of fluorescence intensity following photobleaching of microtubules in wild-type and
397 *capu*^{EY12344}/*spire*^{2F} trans-heterozygous mutant backgrounds. Mutant oocytes initially show similar
398 recovery dynamics to wild-type oocytes, but overall recovers to a lesser degree. N = 5.
- 399 Scale bar: 10 μm (a-f).

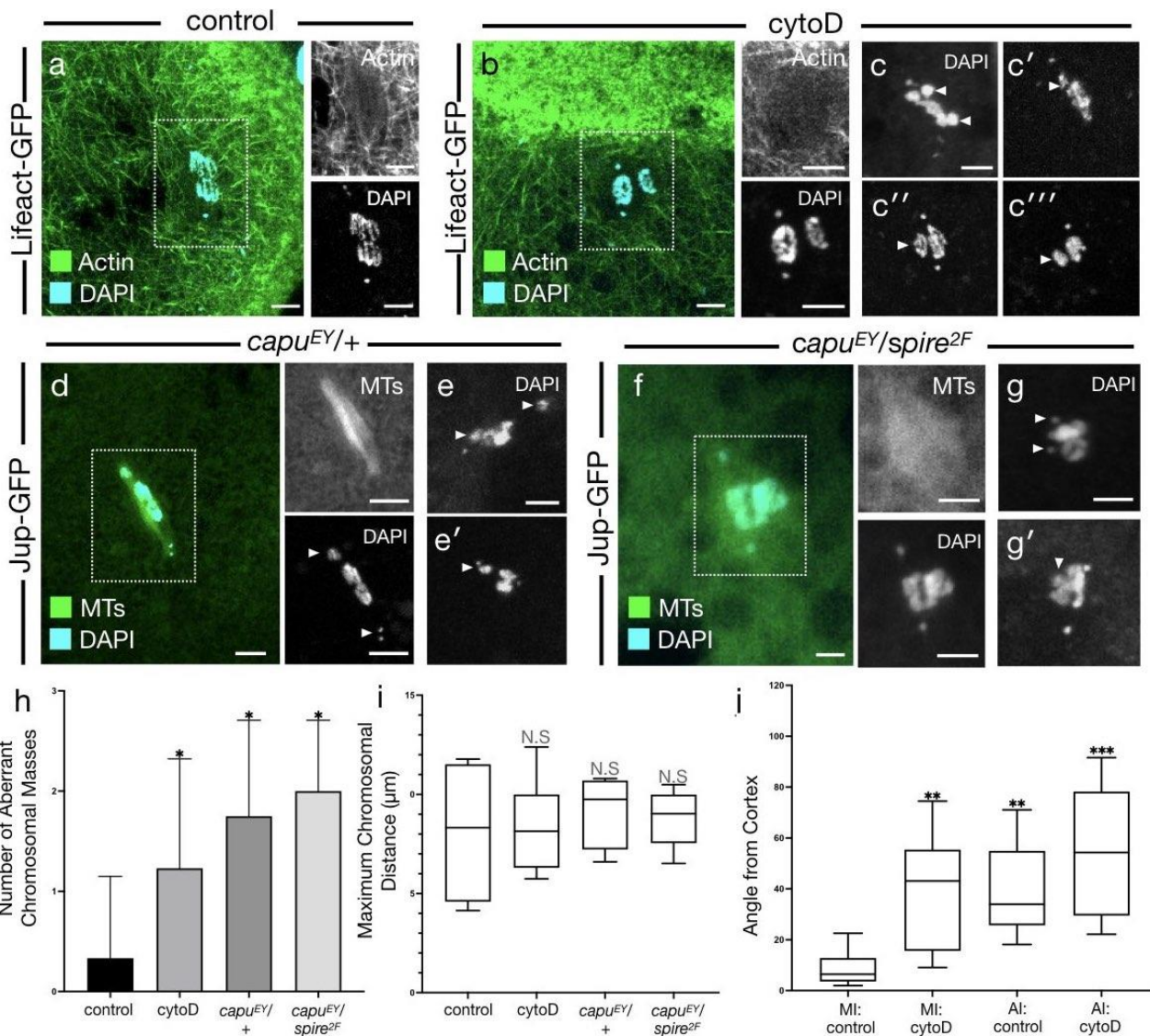
400 **FIGURE 3**



- 401 **Fig. 3** Actin is required for alignment of chromosomes and positioning of the metaphase I spindle.
- 402 a. Confocal Z-projection (10 μm) of a fixed MI oocyte. Merge shows actin (Lifeact-GFP) in green,
- 403 DNA (DAPI) in cyan, demonstrating a spindle-like population of actin surrounding a central
- 404 chromosomal mass. Dashed-line box marks region that is magnified in single-color images to
- 405 right.
- 406 b. Confocal Z-projection (10 μm) of a fixed MI oocyte following incubation with the 10uM of the actin
- 407 depolymerizing agent cytoD. Merge shows actin (Lifeact-GFP) in green, DNA (DAPI) in cyan,
- 408 demonstrating a loss of the spindle-like population of actin and a drastic separation of the
- 409 chromosomal mass into several units that elongate along the spindle axis. Dashed-line box
- 410 marks region that is magnified in single-color images to right.
- 411 c. Confocal Z-projection (10 μm) of a fixed *capu^{EY12344}/+* heterozygous mutant MI oocyte. Merge
- 412 shows actin (Jup-GFP) in green, DNA (DAPI) in cyan, demonstrating a separation of the
- 413 chromosomal mass into two units that begin to migrate along the spindle axis. Dashed-line box
- 414 marks region that is magnified in single-color images to right.
- 415 d. Confocal Z-projection (10 μm) of a fixed *capu^{EY12344}/spire^{2F}* trans-heterozygous mutant MI oocyte.
- 416 Merge shows actin (Jup-GFP) in green, DNA (DAPI) in cyan, demonstrating further separation
- 417 of the chromosomal mass into two distinct units that are migrating to the spindle poles. Dashed-
- 418 line box marks region that is magnified in single-color images to right. Contrasted to better
- 419 visualize the spindle.
- 420 e. Comparison of the maximum chromosomal distance indicates a significant increase in cytoD
- 421 treated and mutant background compared to wild-type. *** < 0.005, * < 0.05, N = 10, student's t-
- 422 test.
- 423 f. Comparison of the spindle-cortex angle (degrees) indicates a significant increase in cytoD
- 424 treated and mutant background compared to wild-type. ** < 0.01, * < 0.05, N = 10, student's t-test.

- 425 g. Schematic representing the MI arrested spindle (g) and anaphase I (AI) spindle (g') in the
426 *Drosophila* oocyte. Microtubules (MTs) are represented in green and chromosomes are
427 represented in blue. MI arrested spindle is narrow with four centrally located chromosomes (g)
428 whereas the AI spindle is has a greater width, chromosomes separating to opposite poles and is
429 rotating relative to the cortex (g')
- 430 h. Confocal Z-projections (10 μm) from a live time series of an MI oocyte pre (h) and post (h')
431 incubation with activation buffer (AB). Spindle-like actin (UtrCH-GFP) appears narrow pre-AB (h)
432 but undergoes a morphological change as it contracts and widens post-AB (h'). N = 10.
- 433 Scale bar: 5 μm (a-d), 10 μm (h).

434 **FIGURE 4**

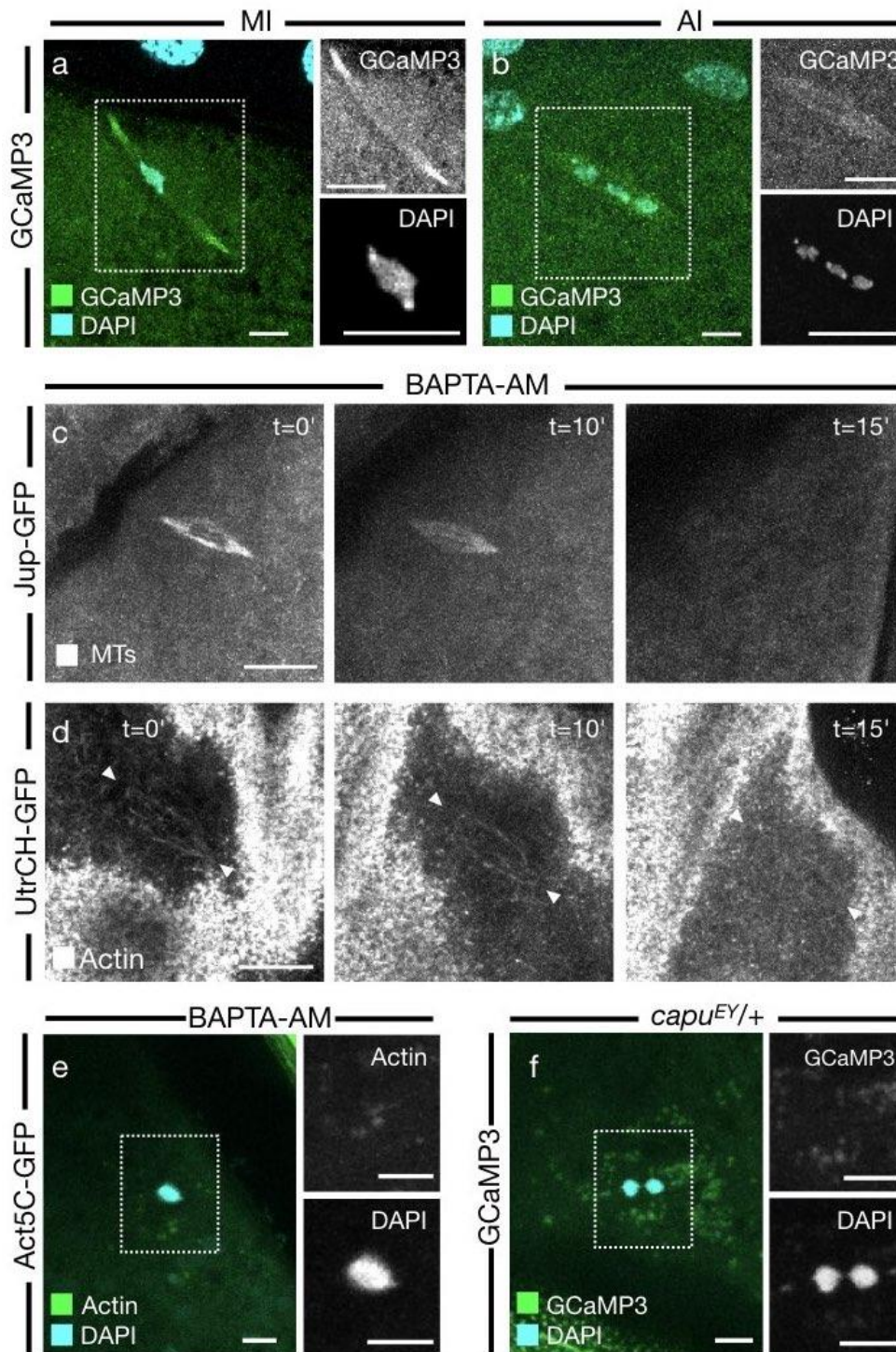


435 **Fig. 4** Actin is required for accurate segregation of chromosomes during anaphase I.

- 436 a. Confocal Z-projection (10 μm) of a fixed AI oocyte. Merge shows actin (Lifeact-GFP) in green,
 437 DNA (DAPI) in cyan, demonstrating a filamentous spindle-like population of actin surrounding
 438 the segregating anaphase chromosomes. Dashed-line box marks region that is magnified in
 439 single-color images to right. N = 15.
- 440 b. Confocal Z-projection (10 μm) of a fixed AI oocyte following incubation with the 10 μM of the
 441 actin depolymerizing agent cytoD. Merge shows actin (Lifeact-GFP) in green, DNA (DAPI) in
 442 cyan, demonstrating the loss of a spindle actin population and the disruption of the accurate
 443 segregation of the chromosomes. Dashed-line box marks region that is magnified in single-color
 444 images to right. N = 10.
- 445 c. Confocal Z-projections (10 μm) of fixed AI oocytes following incubation with the 10 μM of the
 446 actin depolymerizing agent cytoD (C-C'''). Chromosomes (DAPI) demonstrating further examples
 447 of the variety of disrupted chromosome segregation phenotypes, many showing chromosomal
 448 units separated from the main mass (white arrowheads).

- 449 d. Confocal Z-projection (10 μ m) of a fixed *capu*^{EY12344}/+ heterozygous mutant AI oocyte. Merge
450 shows microtubules (Jup-GFP) in green, DNA (DAPI) in cyan, demonstrating the presence of the
451 spindle but mis-regulation of chromosome segregation. Dashed-line box marks region that is
452 magnified in single-color images to right. N = 12.
- 453 e. Confocal Z-projections (10 μ m) of fixed *capu*^{EY12344}/+ heterozygous mutant AI oocytes (e-e').
454 Chromosomes (DAPI) in cyan demonstrating further examples of the variety of disrupted
455 chromosome segregation phenotypes, many showing chromosomal units separated from the
456 main mass (white arrowheads).
- 457 f. Confocal Z-projection (10 μ m) of a fixed *capu*^{EY12344}/*spire*^{2F} trans-heterozygous mutant AI oocyte.
458 Merge shows microtubules (Jup-GFP) in green, DNA (DAPI) in cyan, demonstrating a reduced
459 microtubule signal and mis-regulation of chromosome segregation. Dashed-line box marks
460 region that is magnified in single-color images to right. N = 8.
- 461 g. Confocal Z-projections (10 μ m) of fixed *capu*^{EY12344}/*spire*^{2F} trans-heterozygous mutant AI oocytes
462 (g-g'). Chromosomes (DAPI) in cyan demonstrating further examples of the variety of disrupted
463 chromosome segregation phenotypes, often showing a complete loss of polarity as the 4th non-
464 exchange chromosomes no longer migrate to poles (white arrowheads).
- 465 h. Comparison of the number of aberrant chromosomal masses shows a significant increase in
466 cytoD treated and mutant backgrounds compared to the wild-type. * < 0.05, N = 8, student's t-
467 test.
- 468 i. Comparison of the maximum chromosomal distance shows no significant difference between
469 cytoD treated and mutant backgrounds. N = 8.
- 470 j. Comparison of the angle between the spindle and cortex shows a significant increase in cytoD
471 treated and mutant backgrounds compared to the wild-type. There is no significant differences
472 between cytoD and mutant oocytes. ** < 0.01, *** < 0.005, N = 8.
- 473 Scale bar: 5 μ m (a-g')

474 **FIGURE 5**



475 **Fig. 5** Calcium is required to maintain the metaphase spindle.

- 476 a. Confocal Z-projection (10 μ m) of a fixed MI oocyte. Merge shows calcium (GCaMP3) in green,
477 DNA (DAPI) in cyan, demonstrating a higher calcium signal in the within the spindle.
478 b. Confocal Z-projection (10 μ m) of a fixed AI oocyte. Merge shows calcium (GCaMP3) in green,
479 DNA (DAPI) in cyan, demonstrating a separating chromosomal mass and a wider spindle.

- 480 c. Confocal Z-projections (10 μm) from a live time series of a MI oocyte treated with BAPTA-AM
481 (t=0'). Microtubules (Jup-GFP) first appear as a typical spindle structure and completely
482 depolymerize post-treatment (t=15'). N = 8.
- 483 d. Confocal Z-projections (10 μm) from a live time series of a MI oocyte treated with BAPTA-AM
484 (t=0'). Actin (UtrCH-GFP) first appear as a typical spindle structure and completely depolymerize
485 post-treatment (t=15'). N = 6.
- 486 e. Confocal Z-projection (10 μm) of a fixed MI oocyte. Merge shows actin (Act5C-GFP) in green,
487 DNA (DAPI) in cyan, demonstrating a loss of the actin spindle and round chromosomal mass. N
488 = 6.
- 489 f. Confocal Z-projection (10 μm) of a fixed *capu*^{EY12344/+} heterozygous mutant MI oocyte. Merge
490 shows calcium (GCaMP3) in green, DNA (DAPI) in cyan, demonstrating a loss of the GCaMP3
491 signal in a spindle conformation and separation of the chromosomes into two separate masses.
492 N = 6.
- 493 Scale bar: 5 μm (a,b,e,f), 10 μm (c,d).

494 **REFERENCES**

- 495 1. Handel, M.A. & Schimenti, J.C. Genetics of mammalian meiosis: regulation, dynamics and
496 impact on fertility. *Nat. Rev. Genet.* **11**, 124-136 (2010).
- 497 2. Bennabi, I., Terret, M.E. & Verlhac, M.H. Meiotic spindle assembly and chromosome segregation
498 in oocytes. *J. Cell. Biol.* **215**, 611-619 (2016).
- 499 3. Yi, K. et al. Sequential actin-based pushing forces drive meiosis I chromosome migration and
500 symmetry breaking in oocytes. *J. Cell. Biol.* **200**, 567-576 (2013).
- 501 4. Field, C.M. & Lenart, P. Bulk cytoplasmic actin and its functions in meiosis and mitosis. *Curr.*
502 *Biol.* **21**, 825-830 (2011).
- 503 5. Mori, M. et al. Intracellular transport by an anchored homogeneously contracting F-actin
504 meshwork. *Curr. Biol.* **21**, 606-611 (2011).
- 505 6. Azoury, J., et al. Spindle positioning in mouse oocytes relies on a dynamic meshwork of actin
506 filaments. *Curr. Biol.* **18**, 1514-1519 (2008).
- 507 7. Azoury, J. et al. Symmetry breaking in mouse oocytes requires transient F-actin meshwork
508 destabilization. *Development* **138**, 2903-2908 (2011).
- 509 8. Nixon, V.L. et al. Ca(2+) oscillations promote APC/C-dependent cyclin B1 degradation during
510 metaphase arrest and completion of meiosis in fertilizing mouse eggs. *Curr. Biol.* **12**, 746-750
511 (2002).
- 512 9. Bolcun-Filas, E. & Handel, M.A. Meiosis: the chromosomal foundation of reproduction. *Biol.*
513 *Reprod.* **99**,112-126 (2018).
- 514 10. McLaughlin, J.M. & Bratu, D.P. *Drosophila melanogaster* Oogenesis: An Overview. *Methods*
515 *Mol. Biol.* **1328**, 1-20 (2015).
- 516 11. Hughes, S.E. et al. Female Meiosis: Synapsis, Recombination, and Segregation in *Drosophila*
517 *melanogaster*. *Genetics* **208**, 875-908 (2018).
- 518 12. Giovanni Bosco, T.L.O.-W. The cell cycle during oogenesis and early embryogenesis in
519 *Drosophila*. *Advances in Developmental Biology and Biochemistry* **12**,107-154 (2002).
- 520 13. Theurkauf, W.E. & Hawley R.S. Meiotic spindle assembly in *Drosophila* females: behavior of
521 nonexchange chromosomes and the effects of mutations in the nod kinesin-like protein. *J. Cell.*
522 *Biol.* **116**,1167-1180 (1992).
- 523 14. York-Andersen, A.H. et al. Osmolarity-regulated swelling initiates egg activation in *Drosophila*.
524 *Open. Biol.* **11**, p210067 (2021).
- 525 15. Hu, Q. & Wolfner M.F. The *Drosophila* Trpm channel mediates calcium influx during egg
526 activation. *Proc. Natl. Acad. Sci.* **116**, 18994-19000 (2019).
- 527 16. Endow, S.A. & Komma D.J. Spindle dynamics during meiosis in *Drosophila* oocytes. *J. Cell. Biol.*
528 **137**,1321-1336 (1997).
- 529 17. Majekodunmi, A., Bowen A.O. & Gilliland W.D., Comparative Cytology of Female Meiosis I
530 Among *Drosophila* Species. *G3 (Bethesda)* **10**, 1765-1774 (2020).
- 531 18. Mogessie, B. & Schuh M., Actin protects mammalian eggs against chromosome segregation
532 errors. *Science* **357**, (2017).
- 533 19. Roeles, J. & Tsiavaliaris G. Actin-microtubule interplay coordinates spindle assembly in human
534 oocytes. *Nat. Commun.* **10**, p4651 (2019).
- 535 20. Kelso, R.J., Hudson, A.M. & Cooley L. *Drosophila* Kelch regulates actin organization via Src64-
536 dependent tyrosine phosphorylation. *J. Cell. Biol.* **156**, 703-713 (2002).
- 537 21. Riedl, J. et al., Lifeact: a versatile marker to visualize F-actin. *Nat. Methods* **5**, 605-607 (2008).
- 538 22. Chang, C.W. et al., Anterior-posterior axis specification in *Drosophila* oocytes: identification of
539 novel bicoid and oskar mRNA localization factors. *Genetics* **188**, 883-896 (2011).

- 540 23. Drechsler, M. et al. Optical flow analysis reveals that Kinesin-mediated advection impacts the
541 orientation of microtubules in the *Drosophila* oocyte. *Mol. Biol. Cell* **31**, 1246-1258 (2020).
- 542 24. York-Andersen, A.H. et al. A calcium-mediated actin redistribution at egg activation in
543 *Drosophila*. *Mol. Reprod. Dev.* **87**, 293-304 (2020).
- 544 25. Li, R. et al., Spindle function in *Xenopus* oocytes involves possible nanodomain calcium
545 signaling. *Mol. Biol. Cell* **27**, 3273-3283 (2016).
- 546 26. Nakai, J., Ohkura, M. & Imoto, K. A high signal-to-noise Ca(2+) probe composed of a single
547 green fluorescent protein. *Nat. Biotechnol.* **19**, 137-141 (2001).
- 548 27. Aaboud, M. et al., Measurement of the Inelastic Proton-Proton Cross Section at $\sqrt{s}=13$ TeV
549 with the ATLAS Detector at the LHC. *Phys. Rev. Lett.* **117**, p182002 (2016).
- 550 28. Descazeaud, V. et al., Calcineurin regulation of cytoskeleton organization: a new paradigm to
551 analyse the effects of calcineurin inhibitors on the kidney. *J. Cell. Mol. Med.* **16**, 218-227 (2012).
- 552 29. Kaneuchi, T. et al. Calcium waves occur as *Drosophila* oocytes activate. *Proc. Natl. Acad. Sci.*
553 **112**, 791-796 (2015).
- 554 30. Rauzi, M., Lenne, P.F. & Lecuit, T. Planar polarized actomyosin contractile flows control epithelial
555 junction remodelling. *Nature* **468**, 1110-1114 (2010).
- 556 31. Weil, T.T., Parton, R.M. & Davis I. Preparing individual *Drosophila* egg chambers for live imaging.
557 *J Vis Exp.* **60**, (2012).
- 558 32. Mahowald, A.P., Goralski, T.J. & Caulton, J.H. In vitro activation of *Drosophila* eggs. *Dev. Biol.*
559 **98**, 437-445 (1983).